Volume 24, No 4 | International Journal of Radiation Research, October 2026

Impact of thoracic tumor motion on spinal cord radiation dose parameters in interstitial brachytherapy

G. Zhang[1], J. Zhang[1], Z. Huang[2], Y. Han[3*#], B. Yang[1*#]

[1]Department of Oncology, The Affiliated Hospital of Southwest Medical University, Luzhou, China
[2]School of Medical Information and Engineering, Southwest Medical University, Luzhou, China
[3]Department of Oncology, The Affiliated Traditional Chinese Medicine Hospital of Southwest Medical University, Luzhou, China

► ***Original article***

Corresponding authors:
Bo Yang, M.D.,
Yunwei Han, Ph.D.
E-mail: *yangbo_lz@163.com, 530018842@qq.com*

Received: February 2025
Final revised: December 2025
Accepted: June 2026

Int. J. Radiat. Res., October 2026; 24(4): 1143-1149

DOI: 10.61186/ijrr.24.4.27

Keywords: *Interstitial Radiotherapy, Lung, Neoplasms, Spinal Cords, Target, Movement.*

[#]These authors have contributed equally to this work.

ABSTRACT

Background: In thoracic tumor radiotherapy, tumor movement with respiration can affect dose distribution, potentially complicating the assessment of dose delivery to organs at risk (OAR). However, no standardized evaluation methods have been reported. We aimed to evaluate the dose–response effects caused by target movement and propose a more accurate method for assessing spinal cord dose in interstitial brachytherapy. ***Materials and Methods:*** Computed tomography (CT) data from 14 patients with lung cancer undergoing interstitial brachytherapy were used to design a distance-change model: $f(d)=a\times e^{bd}$. In this model, the distance (d) between the spinal cord and the clinical target volume (CTV) was defined, and f(d) represented spinal cord radiation dose parameters, including the maximum spinal cord dose (Dmax), dose to 1 cm^3 (D1cc), dose to 0.1 cm^3 (D0.1cc), and dose to 1% of the volume (D1%). Each parameter was fitted separately, assuming that the CTV exhibited simple harmonic oscillation. An experiment was designed to measure the effect of radiation source movement on point dose. ***Results:*** The coefficient of determination (R^2) for the exponential fitting curves of all dose variables exceeded 0.90. Specifically, the R^2 value was 0.94 for Dmax and 0.95 for D1cc, D0.1cc, and D1%. The significance of f(d) was evaluated using the F-test, with $p<0.05$ considered statistically significant. The F-values for Dmax, D1cc, D0.1cc, and D1% were 2,362.63, 3,158.41, 2,705.33, and 2,604.93, respectively, all with $p<0.01$. ***Conclusion:*** Reliance on static CT images in radiotherapy planning systems may result in inaccurate spinal cord dose estimates.

INTRODUCTION

In patients with lung tumors who are not eligible for surgery, intensity-modulated radiation therapy (IMRT), stereotactic body radiation therapy (SBRT), and similar modalities are relatively mainstream radiation therapies [1, 2]. However, external beam radiotherapy (EBRT) requires expensive equipment, such as medical linear accelerators (LAs). The western region of China, which is classified as an underdeveloped area, has a relatively small number of accelerators [3]. Consequently, radiation therapy units in the region have transitioned to delivering internal radiotherapy for thoracic tumors, specifically short-range interstitial brachytherapy, through the purchase of afterloading treatment systems [3, 4].

A recent study involving 75 patients with lung tumors treated with interstitial brachytherapy, reported a median overall survival (OS) of 38.0 months (5-year OS, 44.5%; 95% confidence interval, 33.8–58.6%). Local recurrence-free survival, recurrence-free survival, and distant metastasis-free survival at 5 years were 79.2%, 73.6%, and 50.3%, respectively [1]. These findings have captured the attention of many experts regarding the use of interstitial brachytherapy for lung cancer.

From the perspective of radiotherapy physics, the impact of target area movement on radiation dose in interstitial brachytherapy differs from that in EBRT [5–7]. In EBRT, organ motion affects both the dose delivered to the target and the doses received by organs at risk (OARs). In brachytherapy, particularly 192-iridium interstitial brachytherapy for thoracic tumors, the tumor dose is less affected by organ motion because both the implanted needles and the radiation source move synchronously with the target. However, motion may cause the OARs to move closer to the clinical target volume (CTV) [8–10]. The key distinction is that, in internal radiation, the irradiation range continuously moves [1, 8], whereas in external irradiation, the irradiation field is typically fixed.

In 192-iridium interstitial brachytherapy for thoracic tumors, the spinal cord is often at risk, rendering accurate calculation of the dose delivered to the cord essential. Currently, the dose to the spinal cord is primarily calculated based on the static computed tomography (CT) image obtained using the treatment planning system (TPS) [1, 6, 8]. However, this approach to assessing spinal cord dose has important

[Downloaded from mail.ijrr.com on 2026-11-07]

[DOI: 10.61186/ijrr.24.4.27]

limitations. First, the distance from the spinal cord to the target area may vary between the TPS and the actual treatment. Second, throughout treatment, target motion due to respiration is difficult to mitigate, and this approach does not account for the impact of continuous target movement on the dose delivered to the spinal cord [6]. Few studies have assessed the impact of target motion in interstitial brachytherapy, and there is no consensus on the optimal method for assessing its effect of target motion on spinal cord dose.

In this study, we developed a research plan based on mathematical model assumptions to simulate and analyze the effect of target motion on spinal cord dose. The spinal cord dose parameters included maximum spinal cord dose (Dmax), dose to 1 cm^3 (D1cc), dose to 0.1 cm^3 (D0.1cc), and dose to 1% of the spinal cord volume (D1%), which are commonly used in the literature as indicators of spinal cord maximum dose [11–15]. A harmonic motion experimental device was designed to simulate respiratory motion. Then, the conclusions derived from the mathematical model were validated using this experimental setup.

MATERIALS AND METHODS

Interstitial brachytherapy plans and devices

CT data sets from 14 patients with lung tumors who underwent high-dose-rate 192-iridium afterloading percutaneous interstitial brachytherapy (microSelectron-HDR, Elekta, Stockholm, Sweden) were collected from January 2022 to December 2023 (table 1). The patients had a single solid tumor in the chest, located <100 mm from the spinal cord. All the procedures in this study adhered to the ethical standards set by the Southwest Medical University Affiliated Hospital Committee (Register No. ChiCTR-ONC-12002715) on human experimentation and with the principles of the Helsinki Declaration of 1975, as revised in 2000. All patients provided written informed consent before initiating treatment. Using CT (Lightspeed Plus 4, General Electric Company, Boston, MA, USA) images with a 2.5-mm slice thickness, 14 interstitial brachytherapy plans with a prescribed dose of 10,000 cGy were re-designed in a three-dimensional (3D) radiotherapy TPS (Oncentra 4.3, Elekta). The source dwell positions were placed within the target area with a spacing of 2.5 mm, and the median number of needles implanted was 2 (range, 1–3). A graphical optimization tool in the TPS was utilized, and treatment plans were accepted if they adhered to the following constraints: a minimum dose of 10,000 cGy to 95% of the CTV (D95%) and a lung V20 not exceeding 30%, kept as low as possible.

Spinal cord model

The spinal cord was considered to be a column with a radius of approximately 5 mm [16, 17]. In each CT data set, we designed a cylinder with a radius of 5 mm and a length of approximately 200 mm (the length of spinal cord delineation varied with the number of CT images collected by different patients) to replace the actual spinal cord. Eleven cylinders were used in the spinal cord model. The distances between the spinal cord model and the CTV were set at 0, 5, 10, 15, 20, 25, 30, 40, 50, 100, and 150 mm (figure 1).

Table 1. Patient characteristics.

Characteristic	Frequency (n)/Median (range)
Total patients (n)	14
Sex	
Male	8
Female	6
Location of tumor (n)	
Left lung	9
Right lung	5
CTV (cm^3)	36.46 (4.74–124.50)
Lung volume (cm^3)	2,942.61 (1,988.89-3,943.53)
Spinal cord model volume (cm^3)	16.22 (13.47–21.60)

CTV: clinical target volume.

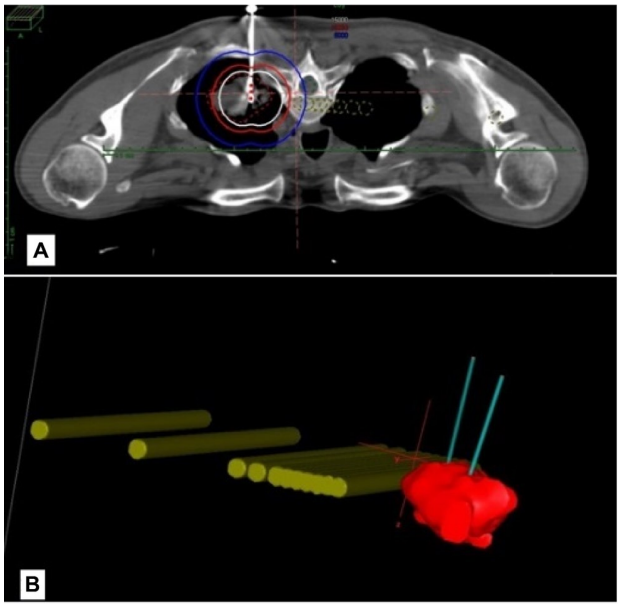


Figure 1. A: Schematic diagram of the spinal cord model and the clinical target volume (CTV). The yellow-green circular dotted lines represent the contours of the spinal cord model with a radius of 5 mm. The solid lines indicate dose curves: white (15,000 cGy), red (10,000 cGy), and blue (5,000 cGy). **B:** Three-dimensional representation of the spinal cord model and the CTV. The CTV is shown in red, while the yellow-green cylinders represent the simulated spinal cord. The blue lines represent the needles inserted into the tumor.

Motion model of the radiation field

As breathing involves reciprocal movement, the CTV moves accordingly with respiration [18–20]. Consequently, the distance between the CTV and the spinal cord in the model varies with this reciprocating motion. In the one-dimensional direction, if the coordinate origin is defined at the spinal cord, the CTV moves relative to the spinal cord.

[Downloaded from mail.ijrr.com on 2026-11-07]

[DOI: 10.61186/ijrr.24.4.27]

Conversely, if the coordinate origin is defined at the CTV, the spinal cord moves relative to the CTV.

In this study, we defined the coordinate origin at the CTV, thereby considering the radiation field as stationary while the spinal cord moved relative to the CTV. Furthermore, the reciprocating motion of the spinal cord was simplified to simple harmonic motion. Accordingly, we assumed the spinal cord followed simple harmonic motion characterized by a center point O, period T, and amplitude A, as illustrated in figure 2.

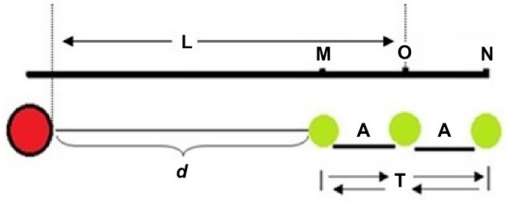


Figure 2. Schematic representation of the spinal cord in simple harmonic motion. The red circle denotes the clinical target volume (CTV), and the yellow-green circles indicate the spinal cord. Point O marks the origin of oscillation, A the amplitude, and d the distance between the spinal cord and the CTV. Point N corresponds to the spinal cord's farthest position from the CTV, while point M corresponds to its nearest position. L represents the distance between the spinal cord and the CTV when the spinal cord is at position O, the equilibrium position of motion. T denotes the period of simple harmonic motion of the spinal cord.

Experimental research on mobile platform

To investigate the effect of continuous target motion on the radiation dose at a certain point, we designed a simple harmonic vibration experiment, in which three needles were placed on a movable platform, and another three needles were placed in parallel with a 10-mm interval. We placed a Farmer-type ionization chamber (PTW-30012, PTW, Freiburg, Germany) connected to a Unidose electrometer (UNIDOS E, PTW) at the M point (50 mm away from the middle needle). A brachytherapy plan (three needles, 40 dwell points, irradiation time: 4 min 58 s, iridium source activity 4.75 Ci) was implemented, and the exposure values to the M point were measured when the platform underwent parallel reciprocating motion with amplitudes of 5 mm, 10 mm, and 15 mm, at a frequency of 16 times/min (figure 3). The exposure doses at the M point were measured three times to obtain an average value, and the differences were compared with different amplitudes.

Theoretical model analysis

In the spinal cord model, the distances between the spinal cord model and the CTV were set to 0, 5, 10, 15, 20, 25, 30, 40, 50, 100, and 150 mm. The maximum spinal cord dose values were recorded calculated by the TPS at these distances, including Dmax, D1cc, D0.1cc, and D1% (figure 4). The distance between the CTV and the spinal cord was defined as *d*. The exponential fitting curve was fitted between the cord dose and *d*. Taking the Dmax as an example, the regression equation for Dmax is defined as follows (equation 1):

$$Dmax = a \times e^{bd} \quad (1)$$

Where; a and b are coefficients to be fitted.

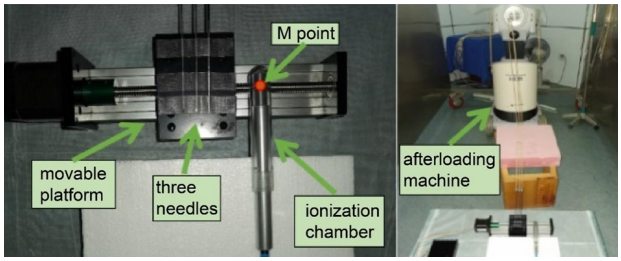


Figure 3. Schematic diagram of the test measurement setup. Three needles are fixed in parallel on the movable platform, and the dose at point M is measured using an ionization chamber.

Taking Dmax as an example, in a stationary radiation field, if the distance between the spinal cord and the CTV is denoted as *d*, the value of Dmax can be calculated using the following formula (equation 2):

$$Dmax = 5{,}523.44e^{-0.030d} \quad (2)$$

Further, if the irradiation time is t_1, the instantaneous dose rate of Dmax is given by $(5{,}523.44e^{-0.030d})/t_1$. The same applies to the D1cc, D0.1cc, and D1%.

Although tumors move with breathing, their CT images remain static in the TPS, making the distance between the tumor and the spinal cord uncertain. Thus, the accuracy of the distance "*d*" in the TPS may be compromised. If the distance reported in the TPS is *d*, the actual distance may instead be *(d + Δd)*.

If the spinal cord is assumed to undergo simple harmonic motion, the actual distance *d* is a variable, defined by the following formula (equation 3).

$$d = L + A\sin(wt) \quad (3)$$

where; $w=2\pi/T$, *L* is the distance from the origin point O to the CTV, *T* is the period, and *A* is the amplitude (Figure 2). Thus, the value of Dmax can be calculated according to the formula (equation 4) at time t1.

$$D_{max} = \int \left(\frac{5523.44}{t1}\right) \times e^{-0.030(L+A\sin wt)} \cdot dt \quad (4)$$

D_{1cc}, $D_{0.1cc}$, and D1% can be expressed similarly, as shown in equations 5, 6, and 7, respectively.

$$D_{1cc} = \int \left(\frac{4334.22}{t1}\right) \times e^{-0.028(L+A\sin wt)} \cdot dt \quad (5)$$

$$D_{0.1cc} = \int \left(\frac{5187.96}{t1}\right) \times e^{-0.029(L+A\sin wt)} \cdot dt \quad (6)$$

$$D_{1\%} = \int \left(\frac{5018.74}{t1}\right) \times e^{-0.030(L+A\sin wt)} \cdot dt \quad (7)$$

Where; t1, *A*, *L*, and *T* are constant.

[Downloaded from mail.ijrr.com on 2026-11-07]

[DOI: 10.61186/ijrr.24.4.27]

According to the fitted exponential formula, the dose values of Dmax, D1cc, D0.1cc, and D1% were calculated integrally when assuming simple harmonic motion of the spinal cord.

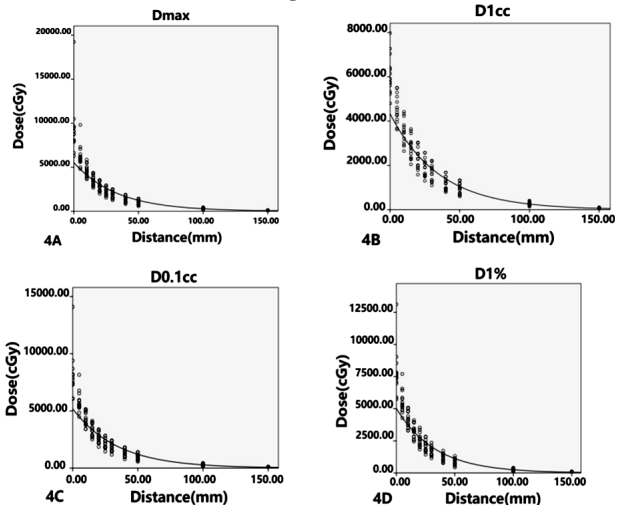


Figure 4. A: Maximum spinal cord dose (Dmax) fitting curve. The exponential fitting formula is: $Dmax=5{,}523.44e^{-0.030d}$ (R^2=0.94; F=2,362.63, p<0.01; a: t=27.31, p<0.01; b: t=−48.61, p <0.01). **B:** Dose received by 1 cm^3 (D1cc) fitting curve. The exponential fitting formula is: $D1cc=4{,}334.22e^{-0.028d}$ (R^2=0.95; F=3,158.41, p<0.01; a: t=33.32, p<0.01; b: t=−56.20, p<0.01). **C:** Dose received by 0.1 cm^3 (D0.1cc) fitting curve. The exponential fitting formula is: $D0.1cc=5{,}187.96e^{-0.029d}$ (R^2=0.95; F=2,705.53, p<0.01; a: t=29.93, p<0.01; b: t=−52.02, p<0.01). **D:** Dose received by 1% (D1%) fitting curve. The exponential fitting formula is: $D1\%=5{,}018.74e^{-0.030d}$ (R^2=0.95; F=2,604.93, P<0.01; a: t=28.61, p<0.01; b: t=−51.04, p<0.01).

Statistical analysis

Utilizing SPSS 19.0 software (IBM Corp, Armonk, NY, USA), the regression coefficients were assessed using the F-test for overall significance and the t-test for individual parameters, with *p*-values <0.05 considered statistically significant. A coefficient of determination (R^2) >0.9 indicated that the model had a good fit.

RESULTS

Results of the fitted exponential equations

The CTV D95% was 10,052.66±12.61 (range: 10,029.28–10,073.98) cGy, and the lung V20 was 18.16±12.38% (range: 5.03%–44.28%). The F-values for Dmax, D1cc, D0.1cc, and D1% were 2,362.63, 3,158.41, 2,705.33, and 2604.93 respectively, p<0.01. Table 2 lists the fitting coefficients and results for the spinal cord dose parameters Dmax, D1cc, D0.1cc, and D1%, while the corresponding fitted curves are presented in figure 4. All R^2 values for the exponential fitting formulas of Dmax, D1cc, D0.1cc, and D1% were >0.94 (table 2, figure 4).

Impact of Positional Uncertainty on Dosage

Table 3 summarizes the dose deviation "Δ" of spinal cord dose metrics, including ΔDmax, ΔD1cc, ΔD0.1cc, and ΔD1%, as a function of positional displacement Δd between the tumor and spinal cord. When the actual tumor-spinal cord distance exceeds that assumed in the TPS by 1 mm (Δd=+1 mm), the fitted model predicted that Dmax was underestimated by up to 2.96% relative to the TPS value. Conversely, when the actual distance was 1 mm shorter than that defined by the TPS (Δd=1 mm), the real value of Dmax might be overestimated by as much as 3.05%.

Table 2. Fitting formula for Dmax, D1cc, D0.1cc, and D1%.

	Fitting formula	R^2	F	*p*	a	t	b	t	*p*
Dmax	$5{,}523.44e^{-0.030d}$	0.94	2,362.63	<0.01	5,523.44	27.31	-0.030	-48.61	<0.01
D1cc	$4{,}334.22e^{-0.028d}$	0.95	3,158.41	<0.01	4,334.22	33.32	-0.028	-56.20	<0.01
D0.1cc	$5{,}187.96e^{-0.029d}$	0.95	2,705.53	<0.01	5,187.96	29.93	-0.029	-52.02	<0.01
D1%	$5{,}018.74e^{-0.030d}$	0.95	2,604.93	<0.01	5,018.74	28.61	-0.030	-51.04	<0.01

Dmax: maximum spinal cord dose, D1cc: dosage received by 1 cm3 of the spinal cord, D0.1cc: dosage received by 0.1 cm3, D1%: dosage received by 1%.

Table 3. Effect of distance uncertainty on spinal cord dose.

					Δd (mm)					
(%)	**-5**	**-4**	**-3**	**-2**	**-1**	**+1**	**+2**	**+3**	**+4**	**+5**
ΔDmax	-16.18	-12.75	-9.42	-6.18	-3.05	2.96	5.82	8.61	11.31	13.93
ΔD1cc	-15.03	-11.85	-8.76	-5.76	-2.84	2.76	5.45	8.06	10.60	13.06
ΔD0.1cc	-15.60	-12.30	-9.09	-5.97	-2.94	2.86	5.64	8.33	10.95	13.50
ΔD1%	-16.18	-12.75	-9.42	-6.18	-3.05	2.96	5.82	8.61	11.31	13.93

Note: ΔDmax represents the percentage influence of distance uncertainty on the Dmax parameter. ΔD1cc represents the percentage influence of distance uncertainty on the D1cc parameter. ΔD0.1cc represents the percentage influence of distance uncertainty on the D0.1cc parameter. ΔD1% represents the percentage influence of distance uncertainty on the D1% parameter. Δd denotes the uncertain distance between the model spinal cord and the clinical target volume. A "+" indicates that the actual distance was larger than the distance provided in the treatment planning system (TPS), while a "-" indicates that the actual distance was smaller than the distance provided in the TPS. Taking ΔDmax as an example, the calculation method is as follows: $[(5523.44e^{-0.030d} - 5523.44e^{-0.030}(d+\Delta d))/5523.44e^{-0.030d}] \times 100\%$. Dmax: maximum spinal cord dose, D1cc: dosage received by 1 cm3 of the spinal cord, D0.1cc: dosage received by 0.1 cm3, D1%: dosage received by 1%.

The corresponding dose deviations in ΔD1cc, ΔD0.1cc, and ΔD1% are reported in table 3 and were calculated using the fitting formulas shown in table 2. The details of the calculation of the dose deviation (Δ) are described in the table footnote.

In the TPS, relative position of the spinal cord to the tumor is determined from static CT imaging acquired at a single time point. During treatment delivery, however, tumor motion may result in deviations from this planned geometry, leading to

[Downloaded from mail.ijrr.com on 2026-11-07]
[DOI: 10.61186/ijrr.24.4.27]

dose overestimation or underestimation to the spinal cord. If the tumor location in the TPS corresponds to its farthest point from the spinal cord, the spinal cord dose may be underestimated; conversely, if it corresponds to the nearest point, the dose may be overestimated.

Quantitative Analysis and Measurement Errors

Assuming t1=60 s, T=3 s, the percentage error of Dmax due to an amplitude of 3 mm was 0.2% when L=5L=5L=5 mm, while an amplitude of 5 mm resulted in a 0.56% error. Table 4 presents the corresponding values for other dose parameters across different amplitudes (A) and distances (L) based on equations 4–7. Furthermore, as shown in table 5, the measured dose at the M point increased with increasing amplitude. The variation patterns of D1cc, D0.1cc, and D1% were highly consistent with those of Dmax.

Comparatively, the magnitude of dose uncertainty to the spinal cord introduced by tumor motion was substantially smaller than that caused by changes in the distance between the spinal cord and the tumor. For example, as indicated by tables 4 and 5, a 2-mm change in distance resulted in a dose deviation of 6.18%, whereas a 2-mm amplitude of tumor motion produced a dose deviation of only 0.09%.

Table 4. Quantitative analysis of the spinal cord radiation dose.

	L (mm)	A (mm)						
		0	1	2	3	5	10	15
Dmax (cGy)	5	4,754.07	4,755.10	4,758.28	4,763.60	4,780.71	/	/
	10	4,091.86	4,092.75	4,095.49	4,100.07	4,114.79	4,184.30	/
	15	3,521.90	3,522.67	3,525.02	3,528.96	3,541.64	3,601.46	3,702.39
	20	3,031.33	3,031.99	3,034.01	3,037.41	3,048.31	3,099.80	3,186.68
	30	2,245.66	2,246.15	2,247.65	2,250.17	2,258.25	2,296.39	2,360.75
	40	1,663.63	1,663.99	1,665.10	1,666.96	1,672.95	1,701.21	1,748.89
	50	1,232.45	1,232.71	1,233.54	1,234.92	1,239.35	1,260.28	1,295.61
	100	275.00	275.06	275.24	275.55	276.54	281.21	289.09
ΔDmax (%)*		0	0.02	0.09	0.20	0.56	2.26	5.12
D1cc (cGy)	5	3,767.99	3,768.70	3,770.89	3,774.57	3,786.37	/	/
	10	3,275.73	3,276.35	3,278.26	3,281.45	3,291.71	3,340.13	/
	15	2,847.79	2,848.32	2,849.98	2,852.76	2,861.67	2,903.77	2,974.69
	20	2,475.75	2,476.21	2,477.65	2,480.07	2,487.82	2,524.42	2,586.07
	30	1,871.13	1,871.48	1,872.57	1,874.39	1,880.25	1,907.91	1,954.51
	40	1,414.17	1,414.44	1,415.25	1,416.64	1,421.07	1,441.97	1,477.19
	50	1,068.81	1,069.01	1,069.63	1,070.67	1,074.02	1,089.82	1,116.43
	100	263.56	263.61	263.77	264.02	264.85	268.75	275.31
ΔD1cc (%)*		0	0.02	0.08	0.17	0.49	1.97	4.45
D0.1cc (cGy)	5	4,487.70	4,488.61	4,491.41	4,496.11	4,511.19	/	/
	10	3,881.96	3,882.75	3,885.17	3,889.23	3,902.28	3,963.86	/
	15	3,357.98	3,358.66	3,360.76	3,364.27	3,375.55	3,428.83	3,518.65
	20	2,904.73	2,905.31	2,907.13	2,910.17	2,919.93	2,966.01	3,043.71
	30	2,173.50	2,173.94	2,175.30	2,177.57	2,184.87	2,219.36	2,277.49
	40	1,626.35	1,626.68	1,627.70	1,629.40	1,634.87	1,660.67	1,704.17
	50	1,216.94	1,217.19	1,217.95	1,219.22	1,223.31	1,242.62	1,275.17
	100	285.46	285.52	285.69	285.99	286.95	291.48	299.12
ΔD0.1cc(%)*		0	0.02	0.08	0.19	0.52	2.11	4.79
D1% (cGy)	5	4,319.67	4,320.61	4,323.49	4,328.33	4,343.87	/	/
	10	3,717.97	3,718.78	3,721.27	3,725.43	3,738.81	3,801.96	/
	15	3,200.08	3,200.78	3,202.92	3,206.51	3,218.02	3,272.38	3,364.09
	20	2,754.34	2,754.94	2,756.78	2,759.86	2,769.77	2,816.56	2,895.50
	30	2,040.47	2,040.91	2,042.27	2,044.55	2,051.90	2,086.56	2,145.04
	40	1,511.60	1,511.94	1,512.95	1,514.60	1,520.08	1,545.76	1,589.08
	50	1,119.83	1,120.07	1,120.82	1,122.08	1,126.11	1,145.12	1,177.22
	100	249.86	249.92	250.09	250.37	251.27	255.51	262.67
ΔD1% (%) *		0	0.02	0.09	0.20	0.56	2.26	5.13

Note: L represents the distance between the model spinal cord and the clinical target volume. A represents the amplitude of the clinical target volume. An amplitude of 0 means that the target was stationary. Δdmax, ΔD1cc, ΔD0.1cc, and ΔD1% represents the percentage errors affected by the amplitude A and compared with data at 0 amplitude. Such as: 0.20%= [(4755.10−4754.07)/4755.10] × 100%. "/": the amplitude of movement surpasses the position of the clinical target volume (CTV). Dmax: maximum spinal cord dose, D1cc: dosage received by 1 cm3 of the spinal cord, D0.1cc: dosage received by 0.1 cm3, D1%: dosage received by 1%.

[Downloaded from mail.ijrr.com on 2026-11-07]

[DOI: 10.61186/ijrr.24.4.27]

Table 5. Measured dose value at the M point.

	A(mm)			
	0	5	10	15
MU (mGy)	11.93±0.05	12.13±0.06	12.62±0.04	12.84±0.05
ΔMU (%)	0	1.67*	5.87	7.63

Note: MU: measurement unit of the Dosimeter; ΔMU were the percentage errors of the MU value affected by the amplitude A compared with the MU value at 0 amplitude; "*": 1.67%= (12.13-11.93)/11.93) ×100%.

DISCUSSION

The effects of thoracic tumor motion on the radiation dose delivered to the spinal cord in brachytherapy have not been previously reported. Sadeghi-Naini *et al.* described that tissue mechanics-based modeling can be employed to effectively characterize lung tumor respiratory motion, improving accuracy in ablative procedures, including brachytherapy [21]. The effects of lung motion on the efficacy of other radiation sources and organ sparing have been investigated. Silva *et al.* reported that spinal cord doses were significantly lower with RapidArc plans than with hybrid RapidArc plans [22]. In patients with non-small cell lung cancer, Ahmed *et al.* found that plans based on four-dimensional (4D) datasets delivered lower doses to the spinal cord and esophagus compared to conventional 3D conformal radiotherapy [23]. Ehrbar *et al.* reported that active motion-management techniques, such as gating or tracking, provided superior tumor dose coverage and better organ sparing, including the spinal cord, compared to passive techniques based on tumor margins [24]. In thoracic SBRT, Ko *et al.* reported that simplified volumetric modulated arc therapy provided less effective dose sparing for critical organs, including the spinal cord, heart, and esophagus, compared to dose-related modulated arc therapy [25].

Tumor movement remains a persistent concern in 192-iridium interstitial brachytherapy for thoracic malignancies. Studies have shown a positive correlation between spinal cord dose and tumor motility, indicating that greater tumor motion is associated with increased spinal cord irradiation [26–29]. Although the placement of interstitial needles may partially constrain tumor movement, this mechanical restriction does not fully mitigate the effects of respiratory-induced motion. Moreover, patient-related factors, including anxiety and episodes of rapid or deep breathing, can further exacerbate tumor motion and contribute to dosimetric uncertainty [30, 31].

Accurate estimation of spinal cord dose should account for two main factors: 1) the spinal cord's location relative to the tumor, and 2) tumor motion. To evaluate spinal cord dose accurately, three key considerations are recommended: 1) measurement of the trajectory and amplitude of CTV motion during calm respiration; 2) verification of the target's movement phase on CT images in the TPS; and 3) ensuring patients maintain steady, relaxed breathing throughout treatment. A simulator or 4D CT is recommended to obtain the amplitude and phase of target motion [32, 33].

This study has certain limitations. First, the simulation does not fully replicate anatomical and biomechanical complexity; for instance, the spinal cord was idealized as a cylindrical structure, and tumor motion was modeled along a single spatial dimension. Future work will address these constraints by incorporating three-dimensional motion models and larger-scale analyses to better reflect clinical conditions. Despite these limitations, the present simulation provides a quantitative estimate of the impact of tumor motion on spinal cord dose variability. These findings enhance understanding of motion-related dosimetric effects in thoracic brachytherapy and may inform strategies to minimize excessive spinal cord irradiation.

CONCLUSIONS

This one-dimensional distance-change model depicting the effect of tumor motion on spinal cord irradiation dose in patients with lung tumors undergoing interstitial brachytherapy demonstrates that tumor motion influences spinal cord doses. An accurate evaluation of the radiation dose to the spinal cord requires not only measurement of the distance between the spinal cord and the tumor but also assessment of the tumor's range of motion. A study on a 3D motion model will be conducted in the next phase of the research plan.

Acknowledgments: The authors would like to express their gratitude to Professor Wu for his valuable advice.

Funding: This study was Supported by Sichuan Science and Technology Program (2026YFMS0152), Sichuan Provice Medical Research Project (S19007), the Key Laboratory Project of Medical Integration and Translational Medicine in Luzhou City (XGY202105, XGY202108).

Conflicts of Interest: The authors declare they have no conflicts of interest.

Author Contributions: B.Y. and Y.H., designed the study. All authors participated in discussing the results, suggesting improvements to the manuscript, and approving the version to be submitted. G.Z., J.Z., and B.Y., implemented the measurements. Z.H., H.Y., and B.Y., analyzed the data. G.Z. and B.Y., wrote the manuscript. All authors read and approved the final manuscript.

REFERENCES

1. Xiang L, Ren PR, Li HX, *et al.* (2023) Effect of 3-dimensional interstitial high-dose-rate brachytherapy with regional metastatic

[Downloaded from mail.ijrr.com on 2026-11-07]

[DOI: 10.61186/ijrr.24.4.27]

lymph node intensity-modulated radiation therapy in locally advanced peripheral non-small cell lung cancer: 5-year follow-up of a phase 2 clinical trial. *Int J Radiat Oncol Biol Phys,* ***115****: 347-355*.
2. Yaprak G, Doğan ÖY, Atasoy Ö, *et al.* (2025) The relationship between lung doses, dosimetric factors, survival, and radiation pneumonitis in lung cancer treated with volumetric-modulated arch therapy and helical tomotherapy. *Int J Radiat Res,* ***23****(3): 535-542*.
3. Huang Na, Peng Xi-Hao, Feng Xi, *et al.* (2021) Investigation and analysis of the current situation and demand of radiotherapy resources in western China in 2019. *Chin J Cancer Prev Treat,* ***28*** *(24): 1882-1887*.
4. Zhang Q, Wang Y, Fang P (2019) Assessment and analysis for deployment appropriateness of medical linear accelerator at hospitals in China. *Chin J Hosp Administr,* ***35****(7): 566-570*.
5. Stroom JC and Heijmen BJ (2002) Geometrical uncertainties, radiotherapy planning margins, and the ICRU-62 report. *Radiother Oncol,* ***64****(1): 75-83*.
6. Yang B, Pang H, Liu X, *et al.* (2021) Influence of CTV movement on the maximal dose of spinal cord for patients with lung cancer undergoing interstitial brachytherapy. *Chin J Cancer Prev Treat,* ***28****: 934-943*.
7. Breen SL, Craig T, Bayley A, *et al.* (2006) Spinal cord planning risk volumes for intensity-modulated radiation therapy of head-and-neck cancer. *Int J Radiat Oncol Biol Phys,* ***64****(1): 321-325*.
8. Yang B, Sun X, Pang H, *et al.* (2020) Determining whether multiple needles are necessary in interstitial brachytherapy for thoracic tumors: A dosimetry analysis. *Indian J Cancer*, ***57****(4): 437-442*.
9. Das RK (1998) Icru 58 (dose and volume specification for reporting interstitial therapy), by international commission on radiation units and measurements. *Med Phys,* ***25****: 1225*.
10. Yang B, Sun X, Pang H, *et al.* (2017) Dosimetric analysis of rib interference of the CTV during interstitial brachytherapy of lung tumors. *J Contemp Brachytherapy*, ***9****(6): 566-571*.
11. Fürweger C, Drexler C, Muacevic A, *et al.* (2014) Cyberknife robotic spinal radiosurgery in prone position: Dosimetric advantage due to posterior radiation access? *J Appl Clin Med Phys,* ***15****(4): 11-21*.
12. Ghia AJ, Guha-Thakurta N, Hess K, *et al.* (2018) Phase 1 study of spinal cord constraint relaxation with single session spine stereotactic radiosurgery in the primary management of patients with inoperable, previously unirradiated metastatic epidural spinal cord compression. *Int J Radiat Oncol Biol Phys,* ***102****(5): 1481-1488*.
13. van der Kogel AJ (1993) Dose-volume effects in the spinal cord. *Radiother Oncol,* ***29****(2): 105-109*.
14. Kirkpatrick JP, van der Kogel AJ, Schultheiss TE (2010) Radiation dose-volume effects in the spinal cord. *Int J Radiat Oncol Biol Phys,* ***76****(3): S42-S49*.
15. Tian X, Shen Z, Wang S, *et al.* (2024) Dosimetric comparison of different radial and longitudinal margins for tomotherapy in esophageal cancer. *Int J Radiat Res,* ***22****(2): 387-393*.
16. Donaldson HH, Davis DJ (2004) Description of charts showing the areas of the cross sections of the human spinal cord at the level of each spinal nerve. *J Comp Neurol,* ***13****(1): 19-40*.
17. Zhang KR, Lu SX, Zheng JZ (Year ????) Cross section area and volume of the spinal cord segments of Chinese. *Acta Anat Sin*, ***11:*** *277-282*.
18. Zhao KL, Liao Z, Bucci MK, *et al.* (2007) Evaluation of respiratory-induced target motion for esophageal tumors at the gastroesophageal junction. *Radiother Oncol,* ***84****(3): 283-289*.
19. Dieleman EM, Senan S, Vincent A, *et al.* (2007) Four-dimensional computed tomographic analysis of esophageal mobility during normal respiration. *Int J Radiat Oncol Biol Phys,* ***67****(3): 775-780*.
20. Yaremko BP, Guerrero TM, McAleer MF, *et al.* (2008) Determination of respiratory motion for distal esophagus cancer using four-dimensional computed tomography. *Int J Radiat Oncol Biol Phys,* ***70****(1): 145-153*.
21. van Sörnsen de Koste JR, Lagerwaard FJ, Nijssen-Visser MR, *et al.* (2003) Tumor location cannot predict the mobility of lung tumors: A 3D analysis of data generated from multiple CT scans. *Int J Radiat Oncol Biol Phys,* ***56****(2): 348-354*.
22. Michalski D, Sontag M, Li F, *et al.* (2008) Four-dimensional computed tomography-based interfractional reproducibility study of lung tumor intrafractional motion. *Int J Radiat Oncol Biol Phys,* ***71****(3): 714-724*.
23. Sadeghi-Naini A, Shirzadi Z, Samani A (2012) Towards modeling tumor motion in the deflated lung for minimally invasive ablative procedures. *Comput Aided Surg,* ***17****(5): 211-220*.
24. Silva SR, Surucu M, Steber J, *et al.* (2017) Clinical application of a hybrid rapidarc radiotherapy technique for locally advanced lung cancer. *Technol Cancer Res Treat,* ***16****(2): 224-230*.
25. Ahmed N, Venkataraman S, Johnson K, *et al.* (2017) Does motion assessment with 4-dimensional computed tomographic imaging for non-small cell lung cancer radiotherapy improve target volume coverage? *Clin Med Insights Oncol,* ***11****: 1179554917698461*.
26. Chan MK, Kwong DL, Tam E, *et al.* (2013) Quantifying variability of intrafractional target motion in stereotactic body radiotherapy for lung cancers. *J Appl Clin Med Phys,* ***14****(5): 140-152*.
27. Plathow C, Ley S, Fink C, et al (2004) Analysis of intrathoracic tumor mobility during whole breathing cycle by dynamic MRI. *Int J Radiat Oncol Biol Phys,* ***59****(4): 952-959*.
28. van Sörnsen de Koste JR, Lagerwaard FJ, Nijssen-Visser MR, *et al.* (2003) Tumor location cannot predict the mobility of lung tumors: A 3D analysis of data generated from multiple CT scans. *Int J Radiat Oncol Biol Phys,* ***56****(2): 348-354*.
29. Michalski D, Sontag M, Li F, *et al.* (2008) Four-dimensional computed tomography-based interfractional reproducibility study of lung tumor intrafractional motion. *Int J Radiat Oncol Biol Phys,* ***71****(3): 714-724*.
30. Rashid A, Pinkawa M, Haddad H, *et al.* (2021) Interstitial single fraction brachytherapy for malignant pulmonary tumours. *Strahlenther Onkol,* ***197****(5): 416-422*.
31. Borot de Battisti M, Denis de Senneville B, Hautvast G, *et al.* (2017) A novel adaptive needle insertion sequencing for robotic, single needle MR-guided high-dose-rate prostate brachytherapy. *Phys Med Biol*, ***62****(10): 4031-4045*.
32. Hashimoto M, Ito Y, Tanaka Y, *et al.* (2023) Four-dimensional dose reconstruction system for lung cancer VMAT treatment: a 4D phantom study. *Int J Radiat Res,* ***21****(3): 469-474*.
33. Tanabe Y, Deguchi T, Kiritani M, *et al.* (2024) Evaluation of statistical prediction model fitting by combining fiducial markers and lung volume for stereotactic body radiotherapy. *Int J Radiat Res*, ***22****(1): 17-22*.

[Downloaded from mail.ijrr.com on 2026-11-07]

[DOI: 10.61186/ijrr.24.4.27]

[DOI: 10.61186/ijrr.24.4.27] [Downloaded from mail.ijrr.com on 2026-11-07]